Can We Evaluate the Effectiveness of Diverting Agent Only by Hydraulic Fracturing Pressure Signals

TongXuan Gu[1], HanYi Wang[1,2*], Shuang Zheng[3]

[1]School of Resources and Safety Engineering, Chongqing University, China
[2]State Key Laboratory of Coal Mine Disaster Dynamics and Control, China
[3]Aramco Americas, Houston, United States

Abstract

In conventional wisdom, the effectiveness of using diverting agent during hydraulic fracturing can be assessed by monitoring pressure, by assuming that successful plugging perforations of larger hydraulic fractures will lead to a jump in treatment pressure, thus diverting injection fluid to other perforations. This study aims to demystify the concept of evaluating the effectiveness of diverter agents through hydraulic fracturing pressure alone. A fully implicit 3D geomechanical fracture simulator is employed to investigate the relationship between open perforation locations and treatment pressure. Simulation results demonstrate that increase in treatment pressure does not necessary mean that the perforations of one hydraulic fracture is plugged, it can also mean that perforations are plugged at different clusters. Thus, an increase in treatment pressure does not guarantee the diversion of injection fluid.

*Corresponding author: hanyi.wang@cqu.edu.cn

Introduction

In horizontal wellbore with multi-stage hydraulic fracturing, it is challenge to create evenly distributed hydraulic fracture due to reservoir heterogeneity and stress interference (Yuan et al., 2021). To address this issue, diverting agents are often employed during hydraulic fracturing. Common diverting agents including dissolvable particles, fibers and pod (Zhao et al., 2020). Diverting agents are injected in the middle of hydraulic fracture operations. Temporarily sealing the perforations of main fractures not only activates underutilized perforation clusters, raises the net fracture pressure, and improves uniform distribution of injection fluid (Aleksandrov et al., 2018; Bist et al., 2023; Liu et al., 2023).

In the application of diverting agents, evaluating their effectiveness is crucial. Often, an increase in treatment pressure after the injection of diverting agents is considered an indication of successful diverting (Wang et al., 2023; Ren et al., 2024; Xiong et al., 2018). Using pressure signal alone to evaluate the effectiveness of diverting agents on-site and adjust the mass/concentration of diverting agents on the fly has become a common practice for field engineers. However, plugging perforations inevitably leads to increase to treatment pressure, however, the location of plugged perforations also matters, which can not be distinguished from pressure signal alone.

This study aims to demystify the concept of evaluating the effectiveness of diverter agents through hydraulic fracturing pressure alone, by using a fully implicit 3D geomechanical fracture simulator to investigate the relationship between open perforation locations and treatment pressure. Our research findings will provide us a more in-depth understanding of the applicability and limitations of pressure signal-based diversion evaluation.

Hydraulic Fracturing Model

This study employs a fully implicit coupled parallel hydraulic fracturing simulator, which is capable of modeling hydraulic fracture propagation, proppant transport and settlement, and fracture closure. For the detailed mathematical formulas used in the simulator and the validation of the simulator, readers can refer to our previous publications (Zheng et al., 2019; Manchanda et al., 2020; Zheng et al., 2020; Zheng, 2021). In this section, we only briefly discuss how to calculate the perforation friction and fluid allocation between each fracture.

Slurry distribution from the wellbore into each cluster is analogous to current flow through a network of resistances and can be modelled using Kirchhoff's second law. Our model assumes the wellbore to be a tank with finite volume (analogous to an electric capacitor) to consider the wellbore storage effects. Compressible fluid flows into the wellbore from surface and flows out of the wellbore into the fractures. Fluid flow out of the wellbore into different fractures is governed by the perforation pressure drop (Δp_{perfi}), well section friction pressure drop ($\Delta p_{sectioni}$), and the pressure in the fractures near the perforations (Δp_{fi}). This fluid distribution model can handle arbitrary directions of fluid flow, which enables us to model a wide range of physical problems including fluid flow from the wellbore into the fracture (injection) and fluid flow out of the fracture into the wellbore (due to a stress shadow effect or production).

If there are n clusters being considered, then one will have $n+1$ more governing equations and n + 1 more unknowns: n equations for fluid distribution and 1 equation for the wellbore storage effect, and n unknowns for cluster flow rates (q_i) and 1 unknown for bottom hole pressure (p_{BHP}).

The flow can be modelled by the mass conservation in the wellbore. Mass conservation in the wellbore indicates that the fluid entering the wellbore equals to the fluid exiting the wellbore plus the fluid stored in the wellbore due to compressibility. The bulk modulus of the fracturing fluid is:

$$K_f = -V_{well}\frac{dP}{dV} = -V_{well}\frac{P_{BHP}-P_{BHP}^{old}}{(\sum_{i=1}^{n} q_i - q_{in})\Delta t} \quad (1)$$

Thus, the mass conservation equation in the wellbore is:

$$P_{BHP} - P_{BHP}^{old} - \frac{K_f}{V_{well}}(q_{in} - \sum_{i=1}^{n} q_i)\Delta t = 0 \quad (2)$$

For each cluster in one stage, the fracture pressure near the perforation points can be expressed as:

$$p_f = p_{BHP} - \Delta p_{section} - \Delta p_{perf} \quad (3)$$

The fracture pressure near the perforation points (p_{fi}) is calculated by taking the average of the pressure values on the immediate face neighbors close to the perforation.

$$p_{fi} = \frac{\sum_{j=1}^{N_{inj}} p_{fj}}{N_{inj}} \quad (4)$$

The wellbore friction pressure drop is calculated using Eq. (5) (Valko & Economides, 1995) or the friction factor method. In the Valko-Economides correlation, the wellbore friction pressure drop is a function of the distance (L_j) that the fluid has to travel from the well head to the perforation location, the wellbore diameter (D), the wellbore flow rate (q_k), and fluid rheology parameters (k, n). The wellbore friction pressure drop is generally much smaller than the perforation pressure drop.

$$\Delta p_{sectioni} = 2^{3n+2}\pi^{-n}k\left(\frac{1+3n}{n}\right)^{n} D^{-(3n+1)}\sum_{j=1}^{i}\left[L_j\left(\sum_{k=j}^{n_c} q_k\right)^{n}\right] \quad (5)$$

The perforation pressure drop is calculated using the turbulent flow correlations as shown in Eq. (6) in which the pressure drop scales quadratically with the cluster flow rate (q_i) (Romero et al., 1995).It is also a function of the fluid density (ρ), number of active perforations (n_{perf}), perforation diameters (d_{perf}), and the discharge coefficient (K_d). The effect of perforation erosion is also taken into account through dynamic change of the discharge coefficient (Romero et al., 1995). Except from the Romero's correlation, friction factor method can also be applied to calculate the perforation pressure drop magnitude.

$$\Delta p_{perfi} = \frac{0.2369\ q_i^2}{n_{perf}^2 d_{perf}^4 K_d^2} \quad (6)$$

Simulation

In this simulation, we compared three cases of hydraulic fracturing. Each case had three perforation clusters, with 12 perforations in each cluster. Case 1 is the base case, where no plugging measures were implemented. Case 2 involved partial plugging, with 4 perforations in each cluster being blocked. Case 3 is the full plugging of a single cluster situation, where all 12 perforations of one cluster were plugged while the other two clusters remained unblocked.

The specifications of the geometric model are 1200m in the x-direction, 1200m in the y-axis direction, and 50m in the z-axis direction. The x, y, and z directions are each divided into 240 grids. The model is composed of three layers. The middle layer has relatively lower stress, while the upper and lower layers have higher stress, which restricts the vertical growth of fractures. The detailed specific parameters of each layer can be found in Table 1. In the numerical simulation, for the porous flow boundary conditions, a fixed gradient of 0 is set in all directions to restrict the pressure change of the fluid at the boundaries. As for the solid mechanics boundary conditions, a fixed displacement of (0, 0, 0) is set in all directions to ensure the boundary rigidity. This setup aims to simplify the model and focus on studying the internal physical processes. We employ 30 - 50 mesh quartz sand as the proppant and slick water as the fracturing fluid. The relevant parameters are listed in Table 2. The slurry injection rate is illustrated in **Fig. 1**, and the total injection time amounts to 900 seconds.

Parameters \ Layer	Upper layer	Middle layer	Lower layer
Top depth of the layer/(m)	2398	2410	2430
Bottom depth of the layer/(m)	2410	2430	2442
Porosity	0.08	0.08	0.08
Permeability/(md)	0.01	0.01	0.01
Minimum horizontal stress/(MPa)	81	61	81
Maximum horizontal stress/(MPa)	86	66	86
Vertical stress/(MPa)	91	71	91
Poisson's ratio	0.297	0.297	0.297
Young's modulus/(GPa)	17.893	17.893	17.893
Fracture toughness/(MPa)	3	3	3

Table 1. Layer parameters

Parameter Category	Value
Proppant Density (kg/m³)	2650
Proppant Diameter (mm)	0.4

Types of Fracturing Fluids	Slickwater
Viscosity of Slickwater (Pa·s)	0.001
Friction Factor	0
Rheology Index	1

Table 2. Proppant and Fracturing Fluid Parameters

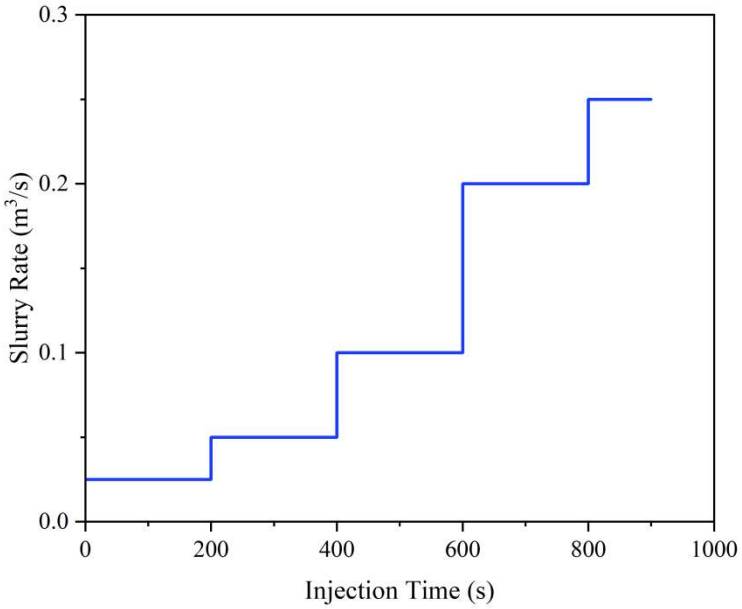

Fig.1. Injection rate during simulation.

Results and Analysis

In Case 1, the number of effective perforations is 12, 12, 12. For Case 2 and Case 3, the numbers of effective perforations are 8, 8, 8 and 0, 12, 12 respectively. In both of these latter two cases, the plugging ratio is one third (12 perforations are plugged, though at different locations for Case 2 and Case 3).

Fig. 2 shows the simulated fracture geometry at the end of the injection for three cases. The difference in length and width distribution are mainly attributed to stress interference and distribution of injection fluid that is affected by number and location of open perforations.

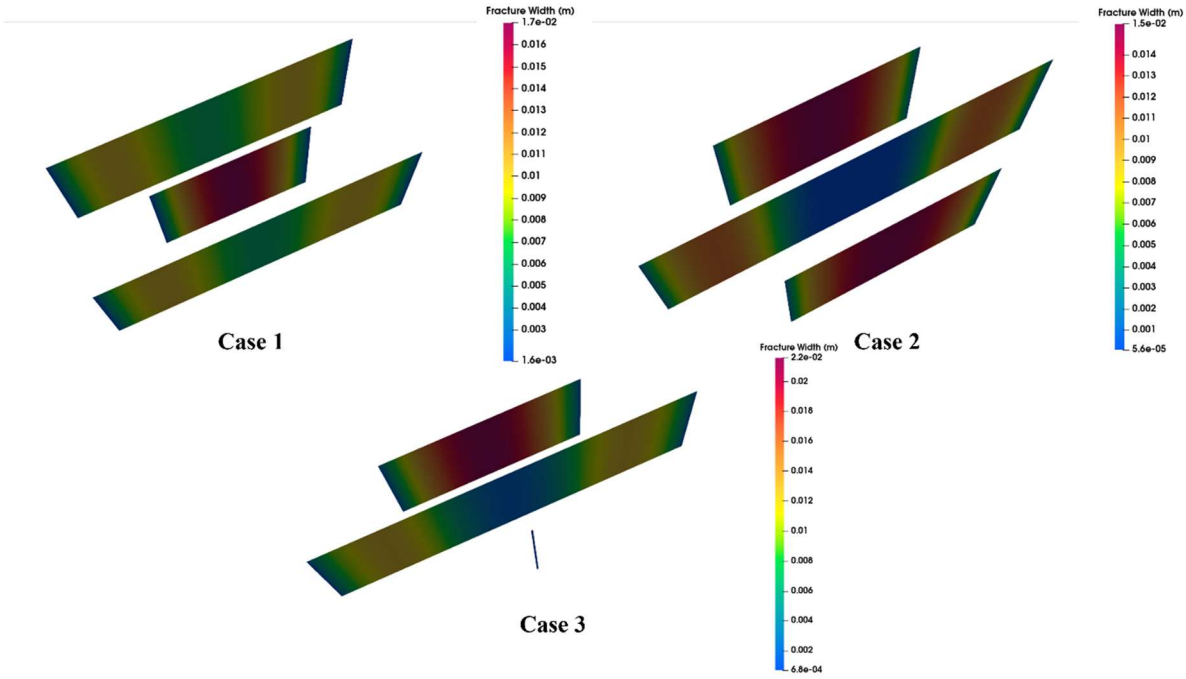

Fig.2. Comparison of fracture geometry at the end of the injection

Fig. 3 shows c evolution of bottom hole pressure throughout the injection phase for three cases. Initially, the pressure curves are very similar, all increases to break down pressure rapidly and then decline sharply. As the injection rate increase, the pressure curves start to separates into different path. It is not surprising that Case 1 has the lowest pressure because it has the largest number of open perforations (i.e., 36 open perforations). The difference between Case 2 and Case 3 is worth very much attention. Remember both Case 2 and Case 3 have 24 open perforations. For Case 3, a single perforation cluster is plugged and fluid is diverted into the other two perforation cluster, resulting two propagating hydraulic fractures. There is no doubt that the pressure of Case 3 should be higher than Case 1. For Case 3, 4 perforations of each perforation cluster is plugged and injection fluid enters three propagating hydraulic fractures, which bottom-hole that is even higher than Case 2.

This is evidence that an increase in fracturing pressure can be achieved by reducing open perforations, but the location of plugged perforations or open perforations cannot be inferred from pressure signal alone. In field practice, the injected diverting agents often randomly plug perforations. They can plug the perforation cluster of large hydraulic fracture thus diverting injection fluid to other smaller hydraulic fractures, or they can plug some perforations of multiple clusters, without diverting injection fluid from larger hydraulic fractures to smaller hydraulic fractures. So it is risk to assess the effectiveness of diverting agent only by observing pressure increase.

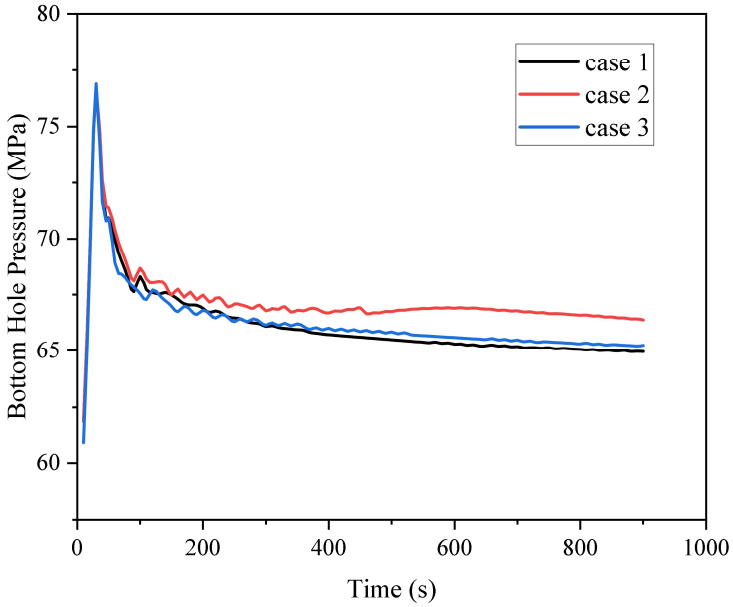

Fig.3. The variation of bottom - hole pressure over injection time.

Even though more case studies or sensitivity studies can be done to supplement the above simulations, to prove a concept correct requires numerous cases for validation, but to prove a concept flawed takes only a single counterexample.

Conclusions

Using pressure signal alone to evaluate the effectiveness of diverting agents on-site and adjust the mass/concentration of diverting agents on the fly is a common practice for field engineers. However, this method is flawed, an increase in fracturing pressure only means some perforations are plugged, it does not guarantee the diversion of injection fluid because the location of plugged perforations cannot be inferred from pressure signal alone. To evaluate the effectiveness of diverting agents with enough confidence, other diagnostic methods (such as distributed fiber optic, micro-seismic measurements, passive or active acoustic measurement, off-set well monitoring, etc.) have to be employed in junction with pressure measurement.

Reference

Aleksandrov, V.M., Galinskij, K., Ponomarev, A.A., Golozubenko, V., & Sivkov, Y.V. (2018). Use of Diverter Compositions for Enhancing the Effectiveness of Oil Recovery from Productive Deposits. Key Engineering Materials, 785, 159 - 170. 10.4028/www.scientific.net/KEM.785.159

Bist, N., Nair, A., Yadav, K., & Sircar, A. (2023). Diverting agents in the oil and gas industry: A comprehensive analysis of their origins, types, and applications. Petroleum Research. https://doi.org/10.1016/j.ptlrs.2023.09.004

Manchanda, R., Zheng, S., Hirose, S., & Sharma, M.M. (2020). Integrating Reservoir Geomechanics with Multiple Fracture Propagation and Proppant Placement. Spe Journal, 25, 662-691. https://doi.org/10.2118/199366-PA

Liu, P., Lou, F., Du, J., Chen, X., Liu, J., & Wang, M. (2023). Impact of key parameters on far-field

temporary plugging and diverting fracturing in fractured reservoirs: A 2D finite element study. Advances in Geo-Energy Research. 10.46690/ager.2023.11.05

Ren, L., Peng, S., Zhao, J., Lin, R., Wu, J., & Wu, J. (2024). Optimization design of plugging agent dosage and application of deep shale gas inner-diversion fracturing. Geoenergy Science and Engineering. https://doi.org/10.1016/j.geoen.2024.212908

Romero, J., Mack, M. G., & Elbel, J. L. (1995). Theoretical Model and Numerical Investigation of Near-Wellbore Effects in Hydraulic Fracturing. Paper presented at the SPE Annual Technical Conference and Exhibition. https://doi.org/10.2118/30506-MS

Valko, P.P., & Economides, M.J. (1995). Hydraulic fracture mechanics.

Wang, D. B., Qin, H., Wang, Y. L., Hu, J. Q., Sun, D. L., & Yu, B. (2023). Experimental study of the temporary plugging capability of diverters to block hydraulic fractures in high-temperature geothermal reservoirs. Petroleum Science, 20(6), 3687-3699. https://doi.org/10.1016/j.petsci.2023.07.002

Xiong, C., Yang, S., Zhou, F., Liu, X., Yang, X., & Yang, X. (2018). High efficiency reservoir stimulation based on temporary plugging and diverting for deep reservoirs. *Petroleum Exploration and Development*. https://doi.org/10.1016/S1876-3804(18)30098-3

Yuan, L., Zhou, F., Li, M., Wang, B., & Bai, J. (2021). Experimental and numerical investigation on particle diverters transport during hydraulic fracturing. Journal of Natural Gas Science and Engineering. https://doi.org/10.1016/j.jngse.2021.104290

Zhao, L., Xiang, C., Honglan, Z., Liu, P., Liang, C., Nanlin, Z., Li, N., Luo, Z., & Juan, D. (2020). A review of diverting agents for reservoir stimulation. *Journal of Petroleum Science and Engineering, 187*, 106734. https://doi.org/10.1016/j.petrol.2019.106734

Zheng, S. (2021). Development of a fully integrated equation of state compositional hydraulic fracturing and reservoir simulator. The University of Texas at Austin. http://dx.doi.org/10.26153/tsw/16954

Zheng, S., Manchanda, R., & Sharma, M.M. (2019). Development of a fully implicit 3-D geomechanical fracture simulator. Journal of Petroleum Science and Engineering. https://doi.org/10.1016/j.petrol.2019.04.065

Zheng, S., Manchanda, R., & Sharma, M. M. (2020). Modeling fracture closure with proppant settling and embedment during shut-in and production. SPE Drilling & Completion, 35(04), 668-683. https://doi.org/10.2118/201205-PA